



HAL
open science

Mapping gas-phase CO₂ in the headspace of two champagne glasses through infrared laser absorption spectroscopy: œnoxpert glass versus inao glass

Vincent Alfonso, Florian Lecasse, Raphael Vallon, Clara Cilindre, Bertrand Parvitte, Virginie Zéninari, Gérard Liger-Belair

► To cite this version:

Vincent Alfonso, Florian Lecasse, Raphael Vallon, Clara Cilindre, Bertrand Parvitte, et al.. Mapping gas-phase CO₂ in the headspace of two champagne glasses through infrared laser absorption spectroscopy: œnoxpert glass versus inao glass. *OENO One*, 2024, 58 (2), 10.20870/oeno-one.2024.58.2.7886 . hal-04643750

HAL Id: hal-04643750

<https://hal.univ-reims.fr/hal-04643750v1>

Submitted on 10 Jul 2024

HAL is a multi-disciplinary open access archive for the deposit and dissemination of scientific research documents, whether they are published or not. The documents may come from teaching and research institutions in France or abroad, or from public or private research centers.

L'archive ouverte pluridisciplinaire **HAL**, est destinée au dépôt et à la diffusion de documents scientifiques de niveau recherche, publiés ou non, émanant des établissements d'enseignement et de recherche français ou étrangers, des laboratoires publics ou privés.



Distributed under a Creative Commons Attribution 4.0 International License



ORIGINAL RESEARCH ARTICLE

Mapping gas-phase CO₂ in the headspace of two champagne glasses through infrared laser absorption spectroscopy: OEnoXpert glass versus INAO glass

Vincent Alfonso, Florian Lecasse, Raphaël Vallon, Clara Cilindre, Bertrand Parvite, Virginie Zéninari and Gérard Liger-Belair*

¹ Université de Reims Champagne-Ardenne, CNRS, GSMA UMR 7331, 51097 Reims, France.

► This article is published in cooperation with OENO Macrowine 2023 (12th international symposium of oenology of Bordeaux and 9th international Macrowine conference), July 10–13 2023, Bordeaux, France.

Guest editors: Philippe Darriet, Pierre-Louis Teissedre and Stéphanie Marchand-Marion.



*correspondence:

gerard.liger-belair@univ-reims.fr

Associate editor:

Markus Herderich



Received:

23 November 2023

Accepted:

22 April 2024

Published:

22 May 2024



This article is published under the **Creative Commons licence** (CC BY 4.0).

Use of all or part of the content of this article must mention the authors, the year of publication, the title, the name of the journal, the volume, the pages and the DOI in compliance with the information given above.

ABSTRACT

Champagne wines are complex hydroalcoholic mixtures supersaturated with dissolved carbon dioxide (CO₂). During tasting, while serving the champagne in a glass and for the few minutes that follow, the headspace of the glass is progressively invaded by many chemical species, including gas-phase CO₂ (likely to disrupt the perception of the wine's bouquet beyond a certain threshold). Real-time monitoring of gas-phase CO₂ was performed through tunable diode laser absorption spectroscopy along a multipoint network in the headspace of two champagne glasses showing distinct shapes and volume capacities (namely, the standard 21 cL INAO glass and the brand new 45 cL OEnoXpert glass, designed by the Union of French Oenologists as a universal glass for the tasting of still and sparkling wines). From the start of the pouring stage and during the several minutes following, a kind of glass type-dependent CO₂ footprint was revealed in the headspace of glasses, which was discussed based on the glass geometry and headspace volume. For an identical volume of champagne dispensed in both glasses, the headspace of OEnoXpert was found to retain gaseous CO₂ more efficiently over time than INAO glass does. Therefore, and extrapolating to aromatic compounds, the chemical space of the OEnoXpert glass should be better preserved throughout the tasting than that of the INAO glass. Moreover, by reducing the volume of champagne served in the glass, the time-dependent CO₂ footprint is significantly reduced in the glass headspace, thus reducing the risk of carbon dioxide burn during tasting.

KEYWORDS: champagne, gaseous CO₂, tasting glasses, CO₂ sensor, TDLAS

INTRODUCTION

The origin of champagne (as a prestigious sparkling wine) dates back to the end of the 17th century (Phillips, 2016). It could then be wrongly imagined that its elaboration and tasting conditions are perfectly controlled today. However, this know-how, dating back over three centuries, continues to benefit from the latest scientific and technical advances in research and development. Indeed, over the past thirty years, numerous research efforts have been carried out to reveal the parameters involved in the bubbling and foaming properties of Champagne and other sparkling wines (Liger-Belair and Cilindre, 2021).

From a chemical point of view, champagne and other sparkling wines can be considered complex hydroalcoholic mixtures saturated with dissolved carbon dioxide (CO₂) (Liger-Belair, 2017). Whatever their production method, sparkling wines are saturated with dissolved CO₂, whether during a second in-bottle fermentation process called *prise de mousse* for premium sparkling wines elaborated according to the traditional method developed in Champagne or through simple exogenous gas-phase CO₂ injection for some cheaper sparkling wines (Gonzalez Viejo *et al.*, 2019). For premium sparkling wines such as Champagne wines, the *prise de mousse* is launched by adding selected yeasts and a certain amount of saccharose (typically about 22–24 g.L⁻¹) inside bottles filled with a base wine and sealed with a crown cap or with a cork stopper (Liger-Belair *et al.*, 2023). During this second alcoholic fermentation, which occurs in cool cellars, the bottles are sealed so that yeast-fermented CO₂ cannot escape and progressively dissolves into the wine. The *prise de mousse* is generally completed within two months, at the end of which the pressure of gas-phase CO₂ in the bottle reaches about 6 bar (at 12 °C). In a sealed bottle of sparkling wine, gas-phase CO₂ and dissolved CO₂ undergo thermodynamic equilibrium according to Henry's law. Under a partial pressure of CO₂ close to 6 bar at 12 °C, it turns out that the wine can dissolve up to 11 – 12 g.L⁻¹ of CO₂ (Liger-Belair and Cilindre, 2021).

In still wine tasting, glass shape was clearly found to influence the perception of aromas (Delwiche and Pelchat, 2002; Hummel *et al.*, 2003). More broadly, the review by Spence and Wan (2015) highlighted how much the sensory perception of a beverage is influenced by the vessel from which it is tasted (including its shape, colour, and material properties, for example). However, when tasting sparkling wines, dissolved and gaseous CO₂ become key parameters throughout the tasting. Indeed, dissolved CO₂ is responsible for bubble nucleation and growth in the glass (Liger-Belair, 2005), as well as for the very characteristic tingling sensation in the mouth (Dessirier *et al.*, 2000; Chandrashekar *et al.*, 2009). Moreover, throughout the tasting of champagne and other sparkling wines, the rising and bursting bubbles act as a continuous paternoster lift to expel gas-phase CO₂ and volatile organic compounds (VOCs) into the headspace of the glass, thus modifying the taster's overall perception of

aromas (Liger-Belair *et al.*, 2009). Nevertheless, it turns out that CO₂ activates the same pain receptors in the deep brain that are activated by tasting spicy food (Wang *et al.*, 2010). Indeed, inhaling a gas space with a concentration of gaseous CO₂ close to 20 % and higher triggers a very unpleasant sting sensation, the so-called “carbonic bite” (Cain and Murphy, 1980; Wise *et al.*, 2003). Once triggered, the carbonic bite completely disrupts both ortho- and retronasal olfactory perception of sparkling wine (Hewson *et al.*, 2009) and, therefore, ultimately, the correct perception of the wine's bouquet.

To reduce the risk of carbonic bite in glasses and ultimately better understand the crucial role of glass shape on the overall perception of a sparkling wine's bouquet, monitoring gas-phase CO₂ in the headspace of various champagne glasses has become a topic of interest over the last dozen years. Indeed, using gas-phase micro-chromatography (μGC), Cilindre *et al.* (2011) were the first to monitor gas-phase CO₂ in the headspace of a glass filled with champagne, but with a low time-resolution (on the order of 0.02 Hz), and at a single point in the headspace of the glass. Gas chromatography revealed CO₂ concentrations, which gradually decreased throughout the first 15 minutes following pouring, with CO₂ concentrations almost twice as high above a tall and narrow flute as above a wider coupe (Liger-Belair *et al.*, 2012). These results are indeed consistent with sensory analyses of Champagne wines conducted by human tasters, as it is generally accepted that the smell of champagne and sparkling wines is more irritating when they are served in a narrow flute than in a wide coupe (Liger-Belair and Cilindre, 2021).

Based on the Tunable Diode Laser Absorption Spectroscopy (TDLAS), a CO₂-Diode Laser Sensor (called the CO₂-DLS) for high-frequency gaseous CO₂ measurements was developed by the authors' research group around fifteen years ago (Mulier *et al.*, 2009). Since then, this instrument has been continuously upgraded and improved (Moriaux *et al.*, 2017; Moriaux *et al.*, 2020; Lecasse *et al.*, 2022). Currently, CO₂-DLS allows real-time monitoring of gas-phase CO₂ in the headspace of champagne glasses under multivariate tasting conditions and with a very high time resolution. The present article addresses the topic of gas-phase CO₂ distribution in the headspace of two different glasses poured with a Champagne wine (the standard and so-called INAO wine glass and the ŒnoXpert glass, recently developed by the Union of French Oenologists). Real-time monitoring of gas-phase CO₂ was performed with the CO₂-DLS, under static tasting conditions, along a multi-point network in the headspace of the two glasses showing distinct shapes and volume capacities. From the start of the pouring stage and during the several minutes following, a kind of glass type-dependent CO₂ footprint was revealed in the headspace of glasses, which was discussed based on the glass geometry and headspace volume. The overall CO₂ footprint is specific to a glass was extrapolated to the dynamics of aromatic compounds and the resulting capacity of a glass to preserve efficiently the wine aromas.

MATERIALS AND METHODS

1. Champagne wine

A batch of standard commercial Champagne wine (Henri de Verlainne, Marne, France), brut labelled, with 12.5 % ethanol by volume, and elaborated in 75 cL bottles with a blend of Pinot Noir and Chardonnay base wines, was used for this set of experiments. Bottles were classically elaborated with 24 g.L⁻¹ of saccharose to launch the *prise de mousse*. After this second in-bottle fermentation, bottles aged on lees in a Champagne cellar for two years (at a temperature close to 12 – 14 °C) before being disgorged and corked with traditional cork stoppers. Before each experiment, bottles were stored in a thermo-regulated wine cellar at 12 ± 1 °C.

2. Glass types and their washing protocol

For this set of experiments, two machine-blown glasses were used and compared with each other. The standard and so-called INAO tasting glass (certified by the Institut National des Appellations d'Origines, with a total volume capacity of 21 cL) was compared with the newly designed and so-called CEnoXpert glass (with a total volume capacity of 45 cL). The INAO is considered by most wine tasters as being a standard glass for still wine tasting. As for the CEnoXpert glass, it was recently designed by the Union of French Oenologists to become the new universal glass reference, suitable for tasting still wines as well as sparkling wines. The two glass types were mass-produced by Lehmann Glass manufacturer (Marne, France).

To trigger a standardised effervescence identical from one glass to another, all glasses were laser-etched on their bottom with a single laser beam point of impact, as described in detail by Liger-Belair (2016). Such laser-etched glasses are usually

easily recognisable, with a central bubbly flow ascending along their axis of symmetry. Before each set of experiments, the glasses were thoroughly washed with an acetic acid solution (10 % v/v), rinsed using distilled water, and then dried in a drying oven at 60 °C. Such a protocol was necessary to remove surface impurities (such as cellulose fibres or tartaric salt crystals) that could trigger heterogeneous nucleation of CO₂ bubbles (Liger-Belair, 2017). Consequently, after such a washing protocol, the formation of bubbles was strictly limited to the small etching made at the bottom of the glasses. Digital images of both glass types are presented in Figure 1 at the same scale.

3. Concentrations of dissolved CO₂ in champagne

Based on the procedure described by Caputi *et al.* (1970), the method officially recommended by the International Organisation of Vine and Wine (labelled OIV-MA-AS314-01) was used to precisely measure the level of dissolved CO₂ in champagne. The concentration of dissolved CO₂ found in champagne samples was determined in two steps. First, in the bottle, just uncorked, but before pouring, the batch of champagne held a concentration of dissolved CO₂, $C_B = 10.75 \pm 0.11$ g.L⁻¹. This is a completely typical concentration for a Champagne wine, which has not aged on lees for several decades (Liger-Belair *et al.*, 2023). Then, and in the same way, dissolved CO₂ concentrations (denoted C_0) were determined immediately after pouring a volume of 50 or 100 mL of champagne (at 12 °C) in the two glass types. To enable a statistical treatment and to provide one single average dissolved CO₂ concentration for each procedure, three services were performed (for each glass type and each volume dispensed).

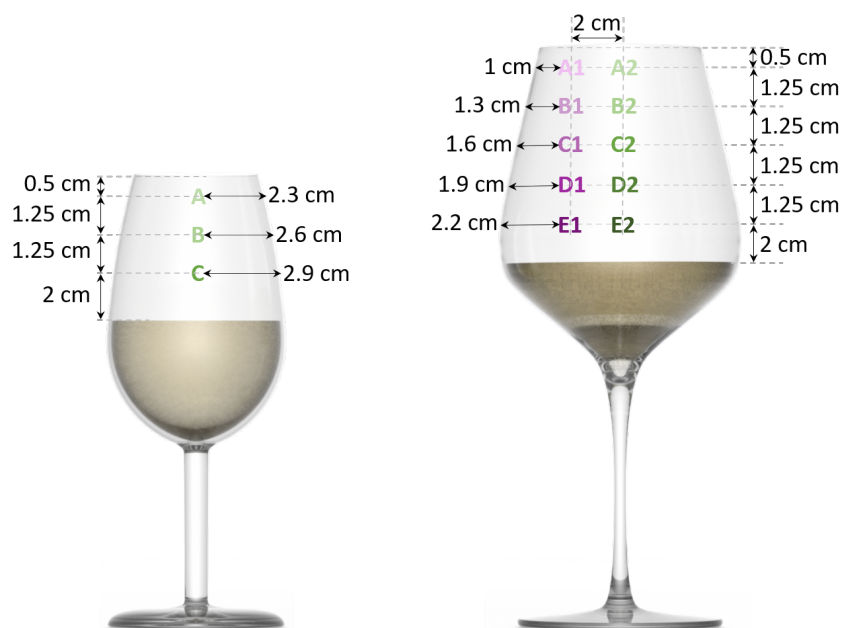


FIGURE 1. Digital scheme of both glass types filled with 100 mL of champagne.

Digital images showing the INAO glass (left) and the CEnoXpert glass (right), with the multipoint network chosen to monitor gas-phase CO₂ in their respective headspaces (as detailed in section 5).

Therefore, the loss of dissolved CO₂ suffered by the wine during the pouring stage (denoted ΔC) finally corresponds to the difference between the concentration of dissolved CO₂ found in the bottle and that found immediately after pouring champagne in the glass (i.e., ΔC = C_B - C₀).

However, it turns out that the ambient air can be considered as a huge thermal tank that quickly warms the gas-phase CO₂ released by champagne during the pouring stage. Therefore, the volume of gas-phase CO₂ desorbing from the liquid phase during the several seconds of the pouring stage (denoted V_{CO₂} and expressed in cm³) can be determined as follows (Moriaux *et al.*, 2021):

$$(1) V_{CO_2} \approx 10^6 \frac{\Delta C V_C R T}{M_{CO_2} P_0}$$

where ΔC is the loss of dissolved CO₂ concentration during the pouring step (expressed in g.L⁻¹), V_C is the volume (in L) of champagne poured into the glass (i.e., 0.1 L or 0.05 L in this work), R is the ideal gas constant (8.31 J.mol⁻¹.K⁻¹), T is the ambient temperature (close to 293 K in our laboratory), M_{CO₂} is the molar mass of CO₂ (44 g.mol⁻¹), and P₀ is the ambient pressure (near 10⁵ Pa).

The various geometrical characteristics of both glasses poured with 50 or 100 mL of champagne are displayed in Table 1, together with their action on the losses of dissolved CO₂ suffered by champagne and the subsequent volume of gaseous CO₂ expelled in the glass headspace during the pouring stage.

TABLE 1. Volume of the glass' headspace, loss of dissolved CO₂ during the service of champagne, and subsequent volume of gas-phase CO₂ expelled above the champagne surface, as determined immediately after pouring 50 or 100 mL of champagne into each glass type.

Glass type	Volume of champagne dispensed (in mL)	Glass' headspace volume (in cm ³)	Loss of dissolved CO ₂ during service (ΔC in g.L ⁻¹)	Volume of gas-phase CO ₂ desorbing during service (V _{CO₂} in cm ³)
INAO	100	110	4.01 ± 0.59*	221.9 ± 32.6*
CEnoXpert	100	350	4.47 ± 0.61*	247.4 ± 33.8*
CEnoXpert	50	400	4.50 ± 0.15*	124.5 ± 4.2*

*Values are means ± standards deviations

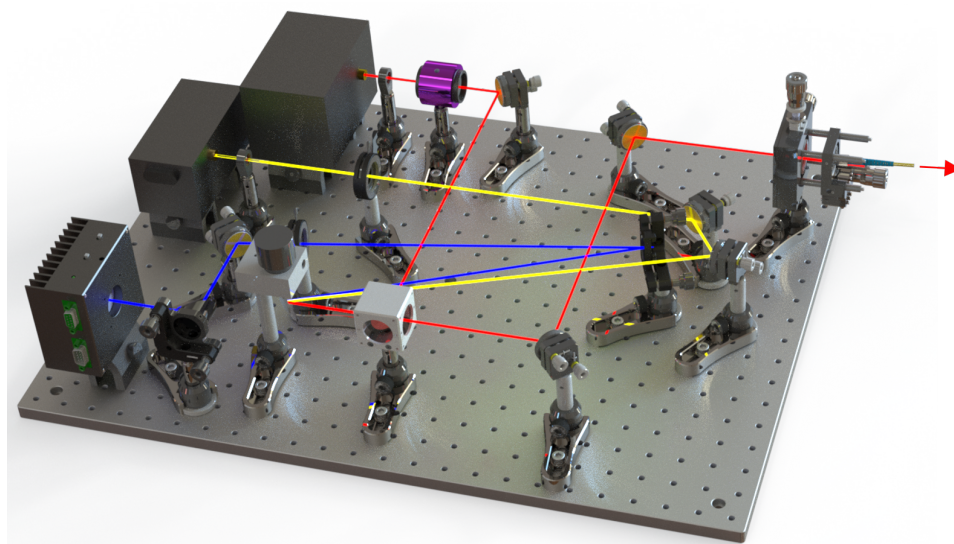


FIGURE 2. Digital 3D sketch of the first optical part of the CO₂-DLS

Digital view of the optical part of the CO₂-DLS, with the blue beam being the optical path of laser #1 (capable of measuring a concentration of gaseous CO₂ ranging from 10 to 100 %), the yellow beam being the optical path of laser #2 (capable of measuring a concentration of gaseous CO₂ ranging from 0 to 10 %), and the red beam being the common path followed by the two laser beams.

4. The CO₂-Diode Laser Sensor

The instrument dedicated to gas-phase CO₂ measurements is based on the Tunable Diode Laser Absorption Spectroscopy design (TDLAS) and was called the CO₂-DLS (Moriaux *et al.*, 2018). Thereby, by including two distributed feedback (DFB) diode lasers emitting at 4985.93 cm⁻¹ and 3728.41 cm⁻¹, respectively, the CO₂-DLS allows the precise measurement of gas-phase CO₂ over a large concentration range from 0.05 % to 100 % (v/v) (Moriaux *et al.*, 2020, 2021). Lasers are selected by using a galvanometric mirror to follow a common path (Lecasse *et al.*, 2022). Once reflected by the mirror, the laser beam is split in two by a pellicle beam splitter (45/55). The first beam goes through a one-inch uncoated germanium Fabry-Pérot to measure the wavenumber shift of lasers, whereas the second beam is guided by an optical fibre to another optical setup aimed at mapping gas-phase CO₂ in the headspace of glasses. The whole optical part with the two DFB diode lasers, the galvanometric mirror, and the beam splitter part (displayed in Figure 2) is placed in a sealed Plexiglas box filled with gas-phase nitrogen to prevent the

laser light from being partly absorbed by the CO₂ naturally present in ambient air.

The second optical setup of the CO₂-DLS, aimed at mapping gas-phase CO₂ in the headspace of glasses, is displayed in Figure 3. It consists of two pairs of galvanometric mirrors, both located at the focal point of an off-axis parabolic mirror positioned on either side of the glass headspace. The role of the first pair of galvanometric mirrors is to scan the glass headspace along both horizontal and vertical axis. Regarding the first parabolic mirror, its role is to reflect the laser beam so that it crosses the headspace of the glass (placed between the symmetrical devices). Once the beam has passed through the headspace of the glass, the second parabolic mirror makes it possible to converge all the incident beams towards the second pair of galvanometric mirrors, whose role is to compensate for the deviation of the beam (induced by the first pair of galvanometric mirrors) to target a cryogenic photodiode. With such a device, monitoring the concentration of gas-phase CO₂ can thus be achieved in the headspace of the glasses, according to a multipoint network defined hereafter, with a 24 ms time resolution per measurement point.

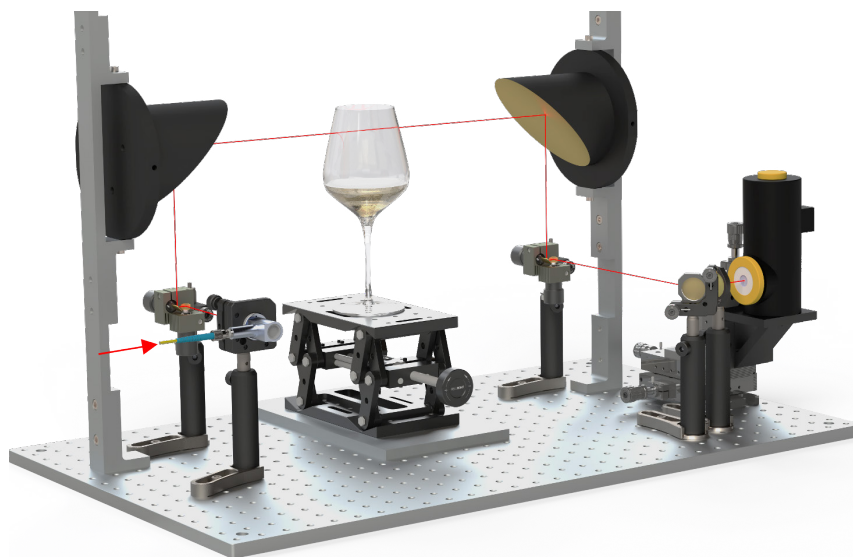


FIGURE 3. Digital 3D sketch of the second optical part of the CO₂-DLS

Digital view of the optical part dedicated to scanning horizontally and vertically the glass headspace with the two pairs of galvanometric mirrors, both located at the focal point of an off-axis parabolic mirror positioned on either side of the glass headspace.

5. The multipoint network in the headspace of glasses

For both glass types, real-time monitoring of gas-phase CO₂ was achieved along a well-defined multipoint network presented in the two digital schemes displayed in Figure 1. Regarding the CenoXpert glass, a two-dimensional (2D) network was determined with five vertically arranged levels separated from 1.25 cm (denoted A, B, C, D, and E, respectively). Each vertical level was structured with two horizontal positions (denoted #1 and #2). Points #2 are vertically arranged along the axis of symmetry of the glass,

while points #1 are offset by 2 cm from the axis of symmetry. Because the glass has a cylindrical symmetry around its axis of symmetry, it was considered unnecessary to select measurement points on either side of this axis of symmetry. Regarding the INAO glass, the multipoint network consists of a single alignment of three vertically arranged levels also separated from 1.25 cm (denoted A, B, and C, respectively). For both glass types, level A is positioned 0.5 cm below the rim (i.e., closest to the taster's nostrils), while levels C (for the INAO) and E (for the CenoXpert) are positioned 2 cm above the liquid surface (for both glass types filled with 100 mL of champagne).

6. Experimental procedure

Measurements were performed in a thermo-regulated room (20 ± 1 °C). The glass (previously level-marked with 50 or 100 mL of distilled water) was placed on the support provided for this purpose between the two parabolic mirrors of the CO₂-DLS, as shown in Figure 3. To obtain experimental baselines for each point of the multipoint tracking defined above (as required for the data processing), the monitoring of CO₂ begins about 30 s before pouring champagne into the glass. The volume of champagne was then carefully poured into the glass to prevent excess foam and the subsequent formation of a liquid film on the glass wall (which may reduce or even cut off the laser beam). Real-time monitoring of gas-phase CO₂ along the multipoint network was carried out within the five minutes following the beginning of the pouring stage. To enable a statistical treatment, three successive pourings from the same bottle were performed for each experimental procedure.

RESULTS AND DISCUSSION

1. How does gas-phase CO₂ evolve, in space and time, in the headspace of the CEnoXpert?

The time dependence of gas-phase CO₂ concentrations along the 2D network of ten points found in the headspace of the CEnoXpert is displayed in Figure 4; within the next five minutes following the beginning of the pouring process, for 100 mL of champagne dispensed at 12 °C. Firstly, and whatever the level at which the monitoring is done in the glass headspace, a rapid increase in the CO₂ concentration was observed during the few tens of seconds following the

start of serving the champagne in the glass until a maximal concentration was reached. This very quick enrichment of the glass headspace in gas-phase CO₂ comes from the massive losses of dissolved CO₂ suffered by champagne when served in the glass (Liger-Belair *et al.*, 2010, 2012). Secondly, after reaching a maximum value (dependent on the measurement level in the headspace), an overall decrease in CO₂ was observed over time, following an exponential decay-type law.

Moreover, the 2D multipoint network chosen to map the temporal evolution of CO₂ in the headspace of the CEnoXpert glass allows a discussion on the vertical and horizontal distributions of CO₂ after serving champagne. Firstly, and unambiguously, the data displayed in Figure 4 show a strong vertical gradient of CO₂ in the headspace of the CEnoXpert glass, with CO₂ concentrations decreasing as one gets closer to the rim of the glass. This observation is consistent with the fact that the source of gaseous CO₂ is obviously the surface of champagne from which dissolved CO₂ progressively escapes, as qualitatively observed by Bourget *et al.* (2013) through infrared imaging. This vertical gradient of gas-phase CO₂ has already been observed in several other glass types, as described by Moriaux *et al.* (2020, 2021). Secondly, it can also be noted from Figure 4 that for the five vertically arranged levels (A, B, C, D, and E), the respective gas-phase CO₂ concentrations found at points #1 (i.e., offset by 2 cm from the axis of symmetry) seem systematically slightly lower than for the points #2 on the axis of symmetry of the glass. Therefore, a slight horizontal gradient in the distribution of gas-phase CO₂ could exist in the headspace of the CEnoXpert glass. More repetitions would nevertheless be needed to reduce error bars and confirm this observation.

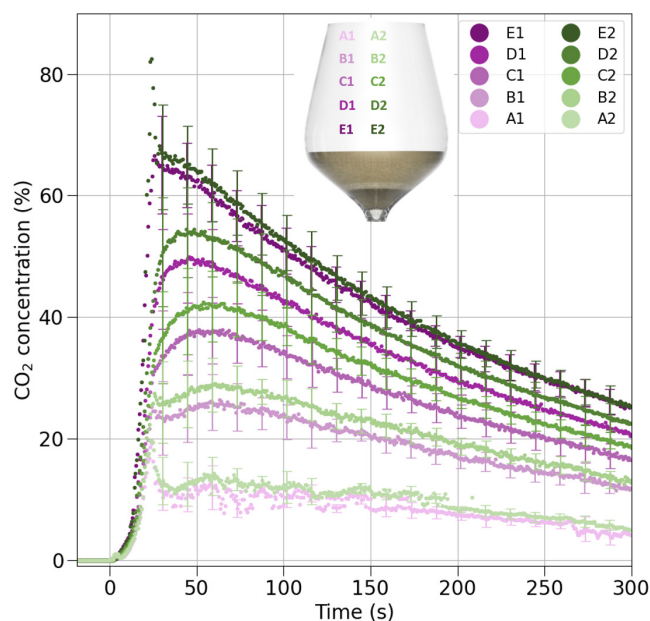


FIGURE 4. Real-time monitoring of gaseous CO₂ (in %) along the 2D network of ten points in the headspace of the CEnoXpert glass.

At $t = 0$, the glass was carefully filled with 100 mL of champagne (at 12 ± 1 °C). The CO₂ time series records resulting from three successive pourings were averaged, with their respective standard deviations displayed every 20 measurement points. The acquisition data frequency is 2.1 Hz.

Notably, in other glass types with much smaller headspace volumes (including the INAO glass), no horizontal gradient of gaseous CO₂ was detected to date, independently of the champagne temperature (Moriaux *et al.* 2020, 2021).

2. Impact of glass shape

For 100 mL of champagne dispensed at 12 °C in both the INAO and CenoXpert glasses, the resulting time dependence of the vertical distribution of gas-phase CO₂ is displayed in Figure 5 (in the headspace, along the axis of symmetry, within the next five minutes following the beginning of the pouring stage). Whatever the type of glass, we find the same overall behaviour regarding gaseous CO₂. After the sharp increase in CO₂ concentration corresponding to the few seconds of the serving stage, the vertical stratification of CO₂ was revealed, with CO₂ concentrations decreasing as one gets closer to the rim of the glass and as time passes. Nevertheless, despite the same overall behaviour, a kind of glass type-dependent CO₂ footprint was revealed, which could be discussed based on the glass geometry and headspace volume.

In champagne glasses, during the pouring stage and after, gas-phase CO₂ desorbs from the wine interface through bubble formation and invisible molecular diffusion (Liger-Belair *et al.*, 2010). Consequently, the greater the glass's air/champagne surface area, the greater the corresponding release of gaseous CO₂ in the glass headspace. Logically, during the pouring stage, the volume of gaseous CO₂ released in the headspace is, therefore, higher for the CenoXpert glass, which has an air/champagne interface of 55 cm² (compared to only 31 cm² for the INAO glass), as shown in Table 1. Moreover, since gaseous CO₂ is approximately 1.5 times denser than dry air, it naturally tends to stagnate in the lower

layers of the headspace of the glass, closest to the surface of the champagne. For the levels closest to the champagne surface (in E2 and C), it is finally not surprising to notice a maximal concentration of gas-phase CO₂ slightly higher in the headspace of the CenoXpert (≈ 73 %) compared with the INAO (≈ 65 %). Conversely, for the levels closest to the rim of glasses (in A2 and A), the maximal concentration of gas-phase CO₂ is much lower for the CenoXpert (≈ 26 %) compared with the INAO (≈ 40 %). Again, this is not surprising. Despite higher volumes of gaseous CO₂ released in the headspace of the CenoXpert glass compared with INAO glass, the headspace volume of CenoXpert (≈ 350 mL) is much higher than the headspace volume of INAO (≈ 110 mL). Therefore, gaseous CO₂ released during the pouring stage can be “diluted” in a much larger volume. In addition, level A2 (closest to the rim of the glass in the CenoXpert) is 7.5 cm from the surface of the wine (which is the source of gaseous CO₂), compared to 5 cm for level A in the case of the INAO glass.

In addition, Figure 5 tells us that the CO₂ decay phase is significantly faster in the headspace of the INAO glass than in the CenoXpert glass. For example, 5 min after the start of serving the champagne in the two glasses, at the levels closest to the rim (i.e., A2 and A), the CO₂ concentration is still ≈ 25 % for the CenoXpert, while it fell to less than 10 % for the INAO. Concretely, this means that the headspace of CenoXpert glass retains gaseous CO₂ more efficiently over time than INAO glass (for the same volume of champagne dispensed). This observation may suggest that, in general, and extrapolating to aromatic compounds, the chemical space of the CenoXpert glass should be better preserved throughout the tasting than that of the INAO glass.

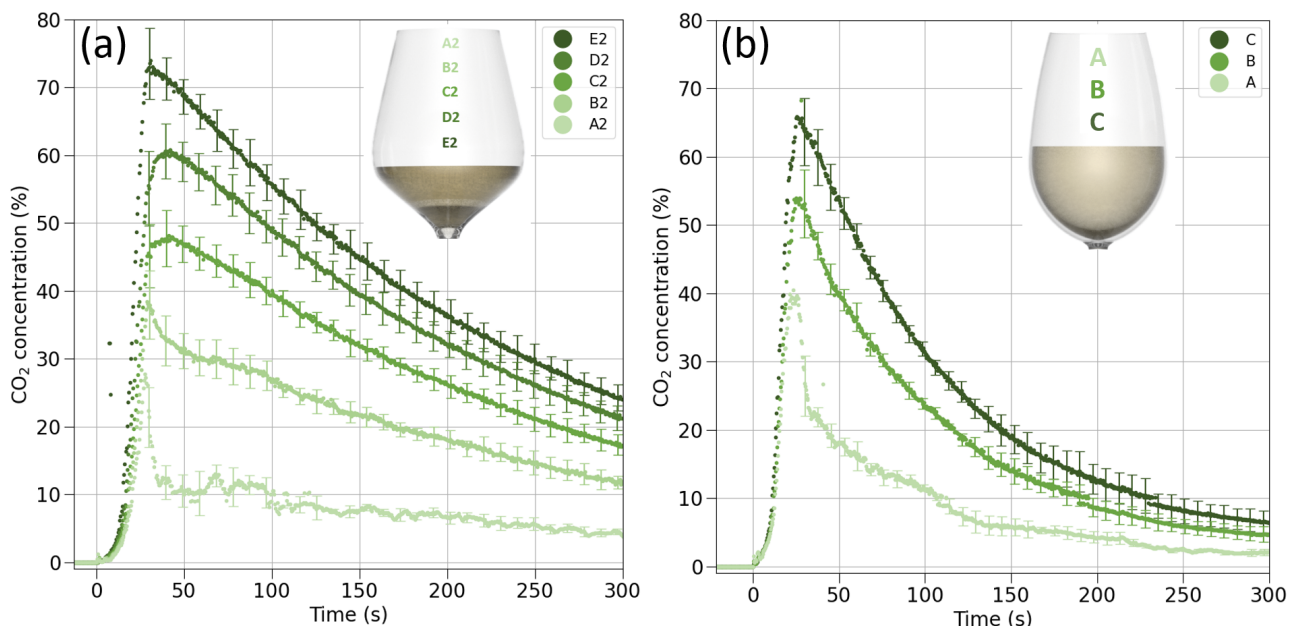


FIGURE 5. Real-time monitoring of gaseous CO₂ (in %) in the headspace of both glass types.

At $t = 0$, the glasses were carefully filled with 100 mL of champagne (at 12 ± 1 °C). Real-time monitoring of CO₂ along five vertically aligned points on the central axis in the headspace of the CenoXpert glass (with a 2.1 Hz data acquisition frequency) (a); real-time monitoring of CO₂ at three vertically aligned points along the central axis in the headspace of the INAO glass (with a 3.5 Hz data acquisition frequency) (b); the CO₂ time series records resulting from three successive pourings were averaged, with their respective standard deviations displayed every 20 measurement points.

Indeed, gas-phase CO₂ is considered one of the many other gaseous species in the headspace of glasses, including volatile organic compounds that also escape from the surface of wine during champagne tasting. The overall dynamics of the CO₂ footprint specific to a glass could, therefore, be extrapolated to the dynamics of other compounds concomitantly desorbing from the wine interface (and thus to the resulting capacity of a glass to preserve more or less efficiently the wine aromas in its headspace).

3. Impact of the volume of wine dispensed

In bars, clubs and restaurants, the volume of champagne commonly dispensed in a glass is 100 mL. This volume indeed corresponds to one alcohol unit (i.e., 10 g of pure ethanol). Nevertheless, during wine-tasting sessions, the

volume dispensed is much closer to 50 mL or less. The influence of the volume of champagne dispensed was also examined regarding how gas-phase CO₂ evolves, in space and time, in the headspace of the CEnoXpert glass. The results are displayed in Figure 6. For better readability of Figure 6, we have only indicated the temporal monitoring of gaseous CO₂ of levels A2 and E2 (i.e., closest to the rim of the glass and closest to the surface of champagne).

Very clearly, the level of champagne dispensed in the glass has a huge impact on the resulting time-dependent CO₂ footprint found in its headspace. At the vertical level E2 in the glass headspace, the maximal concentration of dissolved CO₂ reached after the pouring stage is about twice less for 50 mL than for 100 mL of champagne dispensed. It is even more impressive, closest to the rim at level A2.

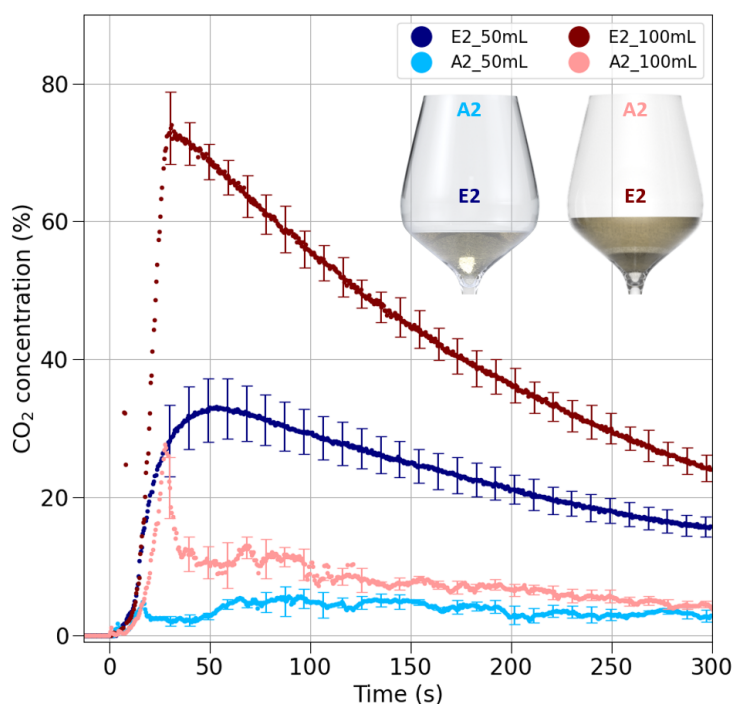


FIGURE 6. Real-time monitoring of gaseous CO₂ (in %) in the headspace of the CEnoXpert filled with 50 mL and 100 mL of champagne, respectively.

At $t = 0$, the glasses were carefully filled with champagne (at 12 ± 1 °C). For both volumes dispensed, gas-phase CO₂ was monitored closest to the glass edge (in A2) and closest to the champagne surface (in E2) (with a 2.1 Hz data acquisition frequency). The CO₂ time series records resulting from three successive pourings were averaged, with their respective standard deviations displayed every 20 measurement points.

Indeed, several factors act concomitantly to drastically reduce the time-dependent CO₂ footprint found in the headspace of the glass dispensed with 50 mL of champagne. First, and as shown in Table 1, the volume of gaseous CO₂ desorbed from champagne during the pouring stage is twice less for 50 mL than for 100 mL of champagne dispensed in the glass. In addition, geometric considerations relating to the glass served with 50 mL of champagne are added to this to explain the drastic reduction of this CO₂ footprint compared to that of a glass served with 100 mL. Indeed, for 50 mL of champagne served, the volume of the glass headspace increases and thus offers a larger volume to dilute the gaseous CO₂ compared to

the glass served with 100 mL. In addition, when the glass is served with 50 mL of champagne, the measurement levels A2 and E2 are therefore located a little higher from the surface of the champagne (which is the physical source of gaseous CO₂ emissions) than when the glass is served at 100 mL. Smaller volumes of champagne served in a glass, therefore, lower the time-dependent CO₂ footprint in the glass' headspace, thereby reducing the risk of carbon dioxide burn during tasting by keeping the concentration of gaseous CO₂ below the carbonic bite threshold limit, which was identified close to 20 % (Cain and Murphy, 1980; Wise *et al.*, 2003).

Finally, careful observation of Figure 6 shows a slight delay in time to reach the maximal concentration of gas-phase CO₂ at level A2 in the headspace, depending on the volume served. Indeed, for a volume of 100 mL of champagne served, from the start of the service, it takes approximately 30 s to reach the maximum CO₂ concentration at level A2. In comparison, for a volume of 50 mL, approximately 50 s are required to reach the maximum CO₂ concentration at the same level in the headspace of the glass (i.e., 20 additional seconds). However, it is worth noting that, for 50 mL served in the glass, the surface of champagne is approximately 1 cm lower compared to the case where 100 mL is served. This additional delay observed in Figure 6 could thus be explained

by the additional diffusion time needed for the CO₂ molecules escaping from the champagne surface to cover the additional distance which separates the surface of the champagne from level A2. The last section of our article offers a more detailed explanation of the phenomenon.

4. A suspected diffusive process in the headspace of the glass

Diffusion is the physical process by which a molecule passes through a medium and spreads out. Diffusion is a consequence of the constant stochastic thermal motion of molecules. Fick's pioneering work made it possible to propose a mathematical formalism to describe these phenomena (Fick, 1855).

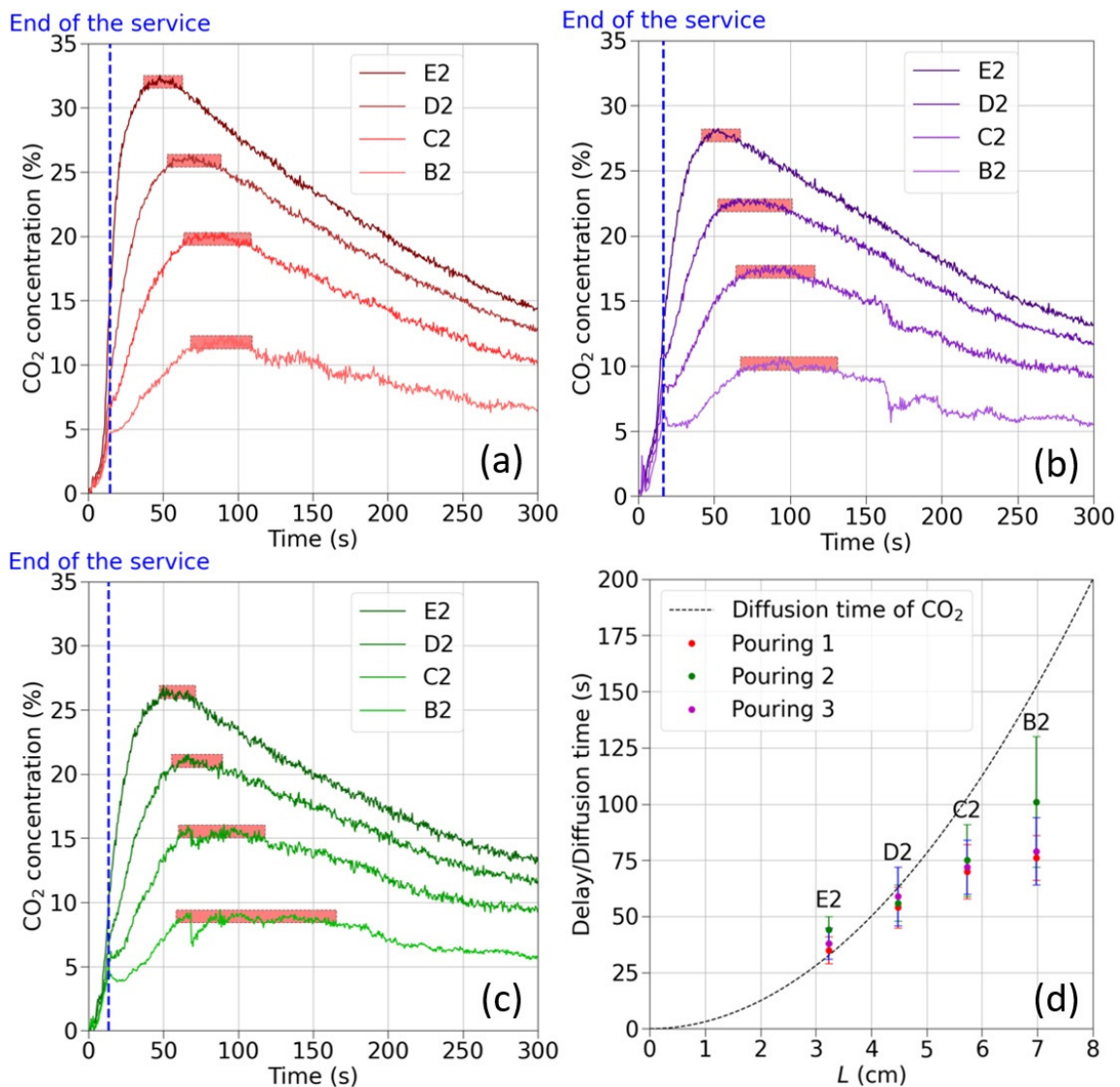


FIGURE 7. Time-dependent CO₂ footprints in the headspace of the CEnoXpert glass resulting from three successive services of 50 mL and the role of diffusion time.

At $t = 0$, the glasses were carefully filled with 50 mL of champagne (at 12 ± 1 °C). During three successive services, real-time monitoring of CO₂ (with a 2.1 Hz data acquisition frequency) along four vertically aligned points on the central axis in the headspace of the CEnoXpert glass (a–c). The end of each service is identified with a blue dotted line. In panel (d), for each service, delay times needed from the end of the service stage to reach the maximum CO₂ concentration are plotted as a function of the distance L to travel between the champagne surface and each measurement level. In panel (d), the theoretical diffusion time needed for a CO₂ molecule to travel a distance L (by pure diffusion) is plotted as a black dotted line.

A statistical physics calculation based on the random walk experienced by a diffusing molecule allows us to write that, during the time t , the one-dimensional root-mean-square distance $\langle z^2 \rangle$ travelled by the molecule from its initial position is ruled by (Di Meglio, 1998):

$$(2) \langle z^2 \rangle \approx 2Dt$$

with D being the diffusion coefficient of the molecular species (expressed in $\text{m}^2 \cdot \text{s}^{-1}$). Note that the diffusion coefficient of gaseous CO_2 in air (at 20°C) is $\approx 1.6 \times 10^{-5} \text{m}^2 \cdot \text{s}^{-1}$ (Massman, 1998).

Therefore, the time scale T (called diffusion time) needed for a molecule to travel a distance L by pure molecular diffusion is given by:

$$(3) T \approx \frac{L^2}{2D}$$

To better understand this observation of a time delay to reach the maximum CO_2 concentrations from one vertical level to another (which could originate from the diffusion of CO_2 molecules in the headspace of the glass), three successive services of 50 mL of champagne have been carried out in the $\text{C}\text{E}\text{N}\text{O}\text{X}\text{p}\text{e}\text{r}\text{t}$ glass. The three respective resulting time-dependent CO_2 footprints are displayed in Figure 7(a–c) (for the levels B2, C2, D2, and E2). The champagne service begins at $t = 0$, and the end of the service is indicated by a blue dotted line. After the end of the champagne service, it appears that the time taken to reach the maximum CO_2 concentration is longer the further the measurement level is from the champagne surface. In Figure 7d, for the three successive services and from the resulting time-dependent CO_2 footprints, the various experimental delay times needed from the end of the service stage to reach the maximum concentration for each measurement level are plotted. Additionally, in Figure 7d, the theoretical diffusion time of CO_2 is also plotted as a function of the distance L to be travelled upwards by CO_2 molecules (by pure diffusion) from their source at the surface of champagne. Figure 7d shows that the theoretical diffusion time needed by a CO_2 molecule to travel the distance from the champagne surface to levels E2 and D2 by pure diffusion is consistent with the delay times observed experimentally. Nevertheless, for levels C2 and B2 closer to the rim of the glass, the theoretical diffusion time seems to become progressively higher than the delay times observed experimentally. One or more other phenomena are probably added to the pure diffusion of CO_2 to finally explain the overall time-dependent CO_2 footprint observed in the glass headspace, including the time delays according to the different levels of measurements to reach the maximum concentration of CO_2 .

To further explore the difference between the theoretical diffusion time of CO_2 and the delays measured experimentally using the CO_2 -DLC in the headspace of the glass, another option to explore could be the role of natural convection. Indeed, the flow of gaseous CO_2 expelled massively upward above the champagne surface during the first seconds of the pouring stage naturally causes convection in the glass' headspace and above. Moreover, the gaseous mixture

expelled above the champagne surface is mainly composed of CO_2 , and its density is greater than that of ambient air. Gravity convection is therefore also suspected in a gas mixture with density inhomogeneities.

Convection should, therefore, also definitely be considered in the glass headspace to better understand the role played by the different parameters on the resulting time-dependent CO_2 footprints left in the headspace of a glass poured with champagne or other sparkling wine. A numerical model that considers the diffusion equations of CO_2 , the upward flow of CO_2 escaping from the champagne surface, gravity convection, and the boundary conditions imposed by the walls of the glass is currently under development.

CONCLUSION

Based on the Tunable Diode Laser Absorption Spectroscopy, a CO_2 -Diode Laser Sensor (CO_2 -DLS) with two distributed feedback (DFB) diode lasers emitting at 4985.93 and 3728.41 cm^{-1} was used to perform real-time monitoring of gas-phase CO_2 along a multi-point network in the headspace of two champagne glasses showing distinct shapes and volume capacities. The standard 21 cL INAO glass was compared with the brand-new 45 cL $\text{C}\text{E}\text{N}\text{O}\text{X}\text{p}\text{e}\text{r}\text{t}$, designed as a universal glass for the tasting of still and sparkling wines. From the start of the pouring stage and during the five minutes following, a glass type-dependent CO_2 footprint, evolving in space and time, was revealed in the headspace of glasses, which was discussed based on the glass geometry and headspace volume.

Unambiguously, our data showed a strong vertical gradient of CO_2 in the headspace of both glasses, with CO_2 concentrations decreasing as one gets closer to the rim of the glass. This observation is consistent with the fact that the source of gaseous CO_2 is obviously the surface of champagne from which dissolved CO_2 progressively escapes. Moreover, the headspace of the $\text{C}\text{E}\text{N}\text{O}\text{X}\text{p}\text{e}\text{r}\text{t}$ glass was found to retain gaseous CO_2 more efficiently over time than the headspace of the INAO glass does (for the same volume of champagne dispensed). Extrapolating to aromatic compounds, this observation may suggest that the chemical headspace of the $\text{C}\text{E}\text{N}\text{O}\text{X}\text{p}\text{e}\text{r}\text{t}$ should be better preserved throughout the tasting than that of the INAO glass. In addition, by reducing the volume of champagne served in the glass, the time-dependent CO_2 footprint was significantly reduced in the glass headspace, thus reducing the risk of carbon dioxide burn during tasting. Finally, to better understand the role played by the different parameters at play on the resulting time-dependent CO_2 footprints left in the headspace of champagne glasses, a numerical model which combines the diffusion equations of CO_2 , natural and gravitational convection, as well as the boundary conditions imposed by the walls of the glass, is currently under development.

This work is considered as being a first step toward a more global approach, combining real-time monitoring of gaseous CO_2 (and VOCs, such as ethanol) in the headspace of various glasses, computational fluid dynamics simulations,

and sensory analysis, with the aim of ultimately better understanding the crucial role of glass shape on the overall perception of sparkling wines' bouquet.

ACKNOWLEDGEMENTS

Thanks are due to Carine Bailleul, cheffe de cave of Champagne Castelnau, for regularly supplying us with champagne samples, and to l'Union des Œnologues de France, for supplying us with various ŒnoXpert glasses.

REFERENCES

- Bourget, M., Liger-Belair, G., Pron, H., & Polidori, G. (2013). Unraveling the release of gaseous CO₂ during champagne serving through high-speed infrared imaging. *Journal of Visualization*, 16(1), 47–52. <https://doi.org/10.1007/s12650-012-0147-9>
- Cain, W.S., & Murphy, C.L. (1980). Interaction between chemoreceptive modalities of odour and irritation. *Nature*, 284, 255–257. <https://www.nature.com/articles/284255a0>
- Caputi, A., Ueda, M., Walter, P., Brown, T., & O-Allo Winery, J. (1970). Titrimetric determination of carbon dioxide in wine. *American Journal of Enology and Viticulture*, 21(3), 140–144. <https://doi.org/10.5344/ajev.1970.21.3.140>
- Chandrashekar, J., Yarmolinsky, D., Von Buchholtz, L., Oka, Y., Sly, W., Ryba, N. J. P., & Zuker, C. S. (2009). The taste of carbonation. *Science*, 326(5951), 443–445. <https://doi.org/10.1126/science.1174601>
- Cilindre, C., Conreux, A., & Liger-Belair, G. (2011). Simultaneous monitoring of gaseous CO₂ and ethanol above champagne glasses via micro-gas chromatography (μGC). *Journal of Agricultural and Food Chemistry*, 59(13), 7317–7323. <https://doi.org/10.1021/jf200748t>
- Delwiche, J.F., & Pelchat, M.L. (2002). Influence of glass shape on wine aroma. *Journal of Sensory Studies*, 17(1), 19–28. <https://doi.org/10.1111/j.1745-459X.2002.tb00329.x>
- Dessirier, J.-M., Simons, C. T., Carstens, M. I., O'mahony, M., & Carstens, E. (2000). Psychophysical and neurobiological evidence that the oral sensation elicited by carbonated water is of chemogenic origin. *Chemical Senses*, 25(3), 277–284. <https://doi.org/10.1093/chemse/25.3.277>
- Di Meglio, J.-M. (1998). Les Etats de la Matière. *Nathan Université, Paris*.
- Fick, A. (1855). On diffusion. *Annalen der Physik*, 170(1), 59–86. <https://doi.org/10.1002/andp.18551700105>
- Gonzalez Viejo, C., Torrico, D. D., Dunshea, F. R., & Fuentes, S. (2019). Bubbles, foam formation, stability and consumer perception of carbonated drinks: A review of current, new and emerging technologies for rapid assessment and control. *Foods*, 8(12), 1–18. <https://doi.org/10.3390/foods8120596>
- Hewson, L., Hollowood, T., Chandra, S., & Hort, J. (2009). Gustatory, olfactory and trigeminal interactions in a model carbonated beverage. *Chemosensory Perception*, 2(2), 94–107. <https://doi.org/10.1007/s12078-009-9043-7>
- Hummel, T., Delwiche, J.F., Schmidt, C., & Hüttenbrink, K.-B. (2003). Effects of the form of glasses on the perception of wine flavors: A study in untrained subjects. *Appetite*, 41(2), 197–202. [https://doi.org/10.1016/S0195-6663\(03\)00082-5](https://doi.org/10.1016/S0195-6663(03)00082-5)
- Lecasse, F., Vallon, R., Polak, F., Cilindre, C., Parvitte, B., Liger-Belair, G., & Zéninari, V. (2022). An infrared laser sensor for monitoring gas-phase CO₂ in the headspace of champagne glasses under wine swirling conditions. *Sensors*, 22(15), 5764. <https://doi.org/10.3390/s22155764>
- Liger-Belair, G. (2005). The physics and chemistry behind the bubbling properties of champagne and sparkling wines: A state-of-the-art review. In *Journal of Agricultural and Food Chemistry*, 53(8), 2788–2802. <https://doi.org/10.1021/jf048259e>
- Liger-Belair, G. (2016). Modeling the losses of dissolved CO₂ from laser-etched champagne glasses. *Journal of Physical Chemistry B*, 120(15), 3724–3734. <https://doi.org/10.1021/acs.jpbc.6b01421>
- Liger-Belair, G. (2017). Effervescence in champagne and sparkling wines: From grape harvest to bubble rise. *European Physical Journal: Special Topics*, 226(1), 3–116. <https://doi.org/10.1140/epjst/e2017-02678-7>
- Liger-Belair, G., Cilindre, C., Gougeon, R. D., Lucio, M., Gebefügi, I., Jeandet, P., & Schmitt-Kopplin, P. (2009). Unraveling different chemical fingerprints between a champagne wine and its aerosols. *Proceedings of the National Academy of Sciences of the United States of America*, 106(39), 16545–16549. <https://doi.org/10.1073/pnas.0906483106>
- Liger-Belair, G., Bourget, M., Villaume, S., Jeandet, P., Pron, H., & Polidori, G. (2010). On the losses of dissolved CO₂ during champagne serving. *Journal of Agricultural and Food Chemistry*, 58(15), 8768–8775. <https://doi.org/10.1021/jf101239w>
- Liger-Belair, G., Bourget, M., Pron, H., Polidori, G., & Cilindre, C. (2012). Monitoring gaseous CO₂ and ethanol above champagne glasses: Flute versus coupe, and the role of temperature. *PLoS ONE*, 7(2). <https://doi.org/10.1371/journal.pone.0030628>
- Liger-Belair, G., & Cilindre, C. (2021). Recent progress in the analytical chemistry of Champagne and sparkling wines. *Annual Review of Analytical Chemistry Annual Rev. Anal. Chem.* 2021, 14, 21–46. <https://doi.org/10.1146/annurev-anchem-061318>
- Liger-Belair, G., Khenniche, C., Poteau, C., Bailleul, C., Thollin, V., & Cilindre, C. (2023). Losses of yeast-fermented carbon dioxide during prolonged champagne aging: Yes, the bottle size does matter! *ACS Omega*, 8(25), 22844–22853. <https://doi.org/10.1021/acsomega.3c01812>
- Massman, W. J. (1998). A review of the molecular diffusivities of H₂O, CO₂, CH₄, CO, O₃, SO₂, NH₃, N₂O, NO, and NO₂ in air, O₂ and N₂ near STP. *Atmospheric Environment*, 32(6), 1111–1127. [https://doi.org/10.1016/S1352-2310\(97\)00391-9](https://doi.org/10.1016/S1352-2310(97)00391-9)
- Moriaux, A. L., Vallon, R., Cilindre, C., Parvitte, B., Liger-Belair, G., & Zeninari, V. (2017). Development and validation of a diode laser sensor for gas-phase CO₂ monitoring above champagne and sparkling wines. *Sensors and Actuator B: Chemical*, 257, 745–752. <https://doi.org/10.1016/j.snb.2017.10.165>
- Moriaux, A. L., Vallon, R., Parvitte, B., Zeninari, V., Liger-Belair, G., & Cilindre, C. (2018). Monitoring gas-phase CO₂ in the headspace of champagne glasses through combined diode laser spectrometry and micro-gas chromatography analysis. *Food Chemistry*, 264, 255–262. <https://doi.org/10.1016/j.foodchem.2018.04.094>
- Moriaux, A. L., Vallon, R., Cilindre, C., Polak, F., Parvitte, B., Liger-Belair, G., & Zeninari, V. (2020). A first step towards the mapping of gas-phase CO₂ in the headspace of champagne glasses. *Infrared Physics and Technology*, 109. <https://doi.org/10.1016/j.infrared.2020.103437>
- Moriaux, A. L., Vallon, R., Lecasse, F., Chauvin, N., Parvitte, B., Zéninari, V., Liger-Belair, G., & Cilindre, C. (2021). How does gas-phase CO₂ evolve in the headspace of champagne glasses? *Journal of Agricultural and Food Chemistry*, 69(7), 2262–2270. <https://doi.org/10.1021/acs.jafc.0c02958>

Mulier, M., Zeninari, V., Joly, L., Decarpenterie, T., Parvitte, B., Jeandet, P., & Liger-Belair, G. (2009). Development of a compact CO₂ sensor based on near-infrared laser technology for enological applications. *Applied Physics B: Lasers and Optics*, *94*(4), 725–733. <https://doi.org/10.1007/s00340-009-3389-z>

Phillips, R. (2016). *French Wine: A History*. University of California Press.

Spence, C., & Wan, X. (2015). Beverage perception and consumption: The influence of the container on the perception

of the contents. *Food Quality and Preference*, *39*, 131-140. <https://doi.org/10.1016/j.foodqual.2014.07.007>

Wang, Y. Y., Chang, R. B., & Liman, E. R. (2010). TRPA1 is a component of the nociceptive response to CO₂. *Journal of Neuroscience*, *30*(39), 12958–12963. <https://doi.org/10.1523/JNEUROSCI.2715-10.2010>

Wise, P. M., Wysocki, C. J., & Radil, T. (2003). Time-intensity ratings of nasal irritation from carbon dioxide. *Chemical Senses*, *28*(9), 751–760. <https://doi.org/10.1093/chemse/bjg065>.